

Solvable model of a polymer in random media with long ranged disorder correlations

Yohannes Shiferaw and Yadin Y. Goldschmidt

*Department of Physics and Astronomy,
University of Pittsburgh, Pittsburgh PA 15260, U.S.A.*

(November 20, 2018)

Abstract

We present an exactly solvable model of a Gaussian (flexible) polymer chain in a quenched random medium. This is the case when the random medium obeys very long range quadratic correlations. The model is solved in d spatial dimensions using the replica method, and practically all the physical properties of the chain can be found. In particular the difference between the behavior of a chain that is free to move and a chain with one end fixed is elucidated. The interesting finding is that a chain that is free to move in a quadratically correlated random potential behaves like a free chain with $R^2 \sim L$, where R is the end to end distance and L is the length of the chain, whereas for a chain anchored at one end $R^2 \sim L^4$. The exact results are found to agree with an alternative numerical solution in $d = 1$ dimensions. The crossover from long ranged to short ranged correlations of the disorder is also explored.

PACS number(s): 05.40-a, 75.10.Nr, 36.20.Ey, 64.60.Cn

I. INTRODUCTION

The behavior of polymer chains in random media is a well studied problem [1-6] that has applications in diverse fields. Besides the polymers themselves this problem is directly related to the statistical mechanics of a quantum particle in a random potential [7], the behavior of flux lines in superconductors in the presence of columnar defects [8,9], and the problem of diffusion in a random catalytic environment [4]. Despite the volume of work that has been done on these problems there are still many unanswered questions. Most of the previous work (with the exception of directed polymers [10,11]) concentrated on disorder with short ranged correlations. In this paper we consider a model with long ranged (quadratic) correlations of the random potential that can serve as a laboratory (toy model) since it can be solved exactly using the replica method [12]. Since some people are somewhat wary of the $n \rightarrow 0$ limit used in replica calculations, we also solve the model numerically in one dimension and obtain an excellent agreement with the analytical solution. More importantly, the numerical solution enables us to explore the crossover from long ranged to short ranged correlations of the disorder and obtain a coherent picture of the behavior of a Gaussian chain in a random medium.

The simplest model of a polymer chain in random media is a Gaussian (flexible) chain [13] in a medium of fixed random obstacles [5]. In this paper we do not include a self-avoiding interaction. This model can be described by the Hamiltonian

$$H = \int_0^L du \left[\frac{M}{2} \left(\frac{d\mathbf{R}(u)}{du} \right)^2 + \frac{\mu}{2} \mathbf{R}^2(u) + V(\mathbf{R}(u)) \right], \quad (1.1)$$

where $\mathbf{R}(u)$ is the d dimensional position vector of a point on the polymer at arc-length u ($0 \leq u \leq L$), and where L is the contour length of the chain. The medium of random obstacles is described by a random potential $V(\mathbf{R})$ that is taken from a Gaussian distribution that satisfies

$$\langle V(\mathbf{R}) \rangle = 0, \quad \langle V(\mathbf{R})V(\mathbf{R}') \rangle = f((\mathbf{R} - \mathbf{R}')^2). \quad (1.2)$$

The harmonic term in the Hamiltonian is included to mimic the effects of finite volume. This is important to ensure that the model is well defined, since it turns out that certain

equilibrium properties of the polymer diverge in the infinite volume limit ($\mu \rightarrow 0$). The function f characterizes the correlations of the random potential, and will depend on the particular problem at hand. The parameter M is inversely proportional to βb^2 , where $\beta = (k_B T)^{-1}$, and where b is the Khun bond step.

Once we have defined the Hamiltonian for any chain configuration $\mathbf{R}(u)$, we can write the partition sum (Green's function) for the set of paths of length L that go from \mathbf{R} to \mathbf{R}' as

$$Z(\mathbf{R}, \mathbf{R}'; L) = \int_{\mathbf{R}(0)=\mathbf{R}}^{\mathbf{R}(L)=\mathbf{R}'} [d\mathbf{R}(u)] \exp(-\beta H). \quad (1.3)$$

All the statistical properties of the polymer will depend on the partition sum. For instance, we can calculate the averaged mean squared displacement of the far end of a polymer with one end that is fixed at the origin. This is a measure of the wandering of a tethered polymer immersed in a random medium. This quantity can be written as

$$\overline{\langle \mathbf{R}_T^2(L) \rangle} = \overline{\left(\frac{\int d\mathbf{R} \mathbf{R}^2 Z(\mathbf{0}, \mathbf{R}; L)}{\int d\mathbf{R} Z(\mathbf{0}, \mathbf{R}; L)} \right)}, \quad (1.4)$$

where the overbar stands for the average of the ratio over the realizations of the random potential. This average is referred to as a quenched average, as opposed to an annealed average, where the numerator and denominator are averaged independently. For a polymer with one end fixed a typical conformation in a random medium is that of a tadpole. The head of the polymer wanders far from the origin to find a region of favorable potential and then the remaining chain settles itself in that region. This is at least what is believed to happen when the disorder has short ranged correlations [3,4]. On the other hand if the chain is not anchored but both ends are free to move, the head to tail mean squared displacement is given by

$$\overline{\langle \mathbf{R}_F^2(L) \rangle} = \overline{\left(\frac{\int d\mathbf{R} d\mathbf{R}' (\mathbf{R} - \mathbf{R}')^2 Z(\mathbf{R}, \mathbf{R}'; L)}{\int d\mathbf{R} d\mathbf{R}' Z(\mathbf{R}, \mathbf{R}'; L)} \right)}. \quad (1.5)$$

In this case the chain can move as a whole to find a favorable environment in the random medium.

In order to compute the quenched average over the random potential we apply the replica method. We first introduce n -copies of the system and average over the random potential to get

$$Z_n(\{\mathbf{R}_a\}, \{\mathbf{R}'_a\}; L) = \overline{Z(\mathbf{R}_1, \mathbf{R}'_1; L) \cdots Z(\mathbf{R}_n, \mathbf{R}'_n; L)} = \int_{\mathbf{R}_a(0)=\mathbf{R}_a}^{\mathbf{R}_a(L)=\mathbf{R}'_a} \prod_{a=1}^n [d\mathbf{R}_a] \exp(-\beta H_n), \quad (1.6)$$

where

$$H_n = \frac{1}{2} \int_0^L du \sum_a \left[M \left(\frac{d\mathbf{R}_a(u)}{du} \right)^2 + \mu \mathbf{R}_a^2(u) \right] - \frac{\beta}{2} \int_0^L du \int_0^L du' \sum_{ab} f((\mathbf{R}_a(u) - \mathbf{R}_b(u'))^2). \quad (1.7)$$

The averaged equilibrium properties of the polymer can now be written in terms of the replicated partition sum $Z_n(\{\mathbf{R}_a\}, \{\mathbf{R}_a\}; L)$. For instance, the mean squared displacement defined in Eq. (1.4) can be written in as

$$\overline{\langle \mathbf{R}_T^2(L) \rangle} = \lim_{n \rightarrow 0} \frac{\int d\mathbf{R}_1 \cdots d\mathbf{R}_n \mathbf{R}_1^2 Z_n(\{\mathbf{0}\}, \{\mathbf{R}_a\}; L)}{\int d\mathbf{R}_1 \cdots d\mathbf{R}_n Z_n(\{\mathbf{0}\}, \{\mathbf{R}_a\}; L)}, \quad (1.8)$$

and similarly

$$\overline{\langle \mathbf{R}_F^2(L) \rangle} = \lim_{n \rightarrow 0} \frac{\int \prod d\mathbf{R}_a \prod d\mathbf{R}'_a (\mathbf{R}_1 - \mathbf{R}'_1)^2 Z_n(\{\mathbf{R}_a\}, \{\mathbf{R}'_a\}; L)}{\int \prod d\mathbf{R}_a \prod d\mathbf{R}'_a Z_n(\{\mathbf{R}_a\}, \{\mathbf{R}'_a\}; L)}. \quad (1.9)$$

Thus, the averaged equilibrium properties of the polymer can be extracted from an n -body problem by taking the $n \rightarrow 0$ limit at the end. This limit has to be taken with care, by solving the problem analytically for general n , before taking the limit of $n \rightarrow 0$.

We now proceed to introduce our toy model that can be exactly solved using the replica method and which also lends itself to an accurate numerical solution. This is the case when a Gaussian polymer chain is immersed in a random medium that has very long range spatial correlations. In particular, we take the correlation function to be of the form

$$\langle V(\mathbf{R})V(\mathbf{R}') \rangle = f((\mathbf{R} - \mathbf{R}')^2) = g(1 - (\mathbf{R} - \mathbf{R}')^2/\xi^2), \quad (1.10)$$

where ξ is chosen to be larger than the sample size, so that the correlation function is well defined (non-negative) over the entire sample. Since this model can be solved exactly using

the replica method, we can compute all the important physical properties of the polymer chain, and then compare the exact analytical results with an alternative numerical solution (at $d = 1$). Also, this model of long range correlations is interesting in its own right in that it may serve as a good approximation to any correlation function f that is smooth and slowly decaying. Most cases investigated so far in the literature are concerned with disorder with short ranged correlations.

There are many properties of the polymer chain that can be exactly computed. In addition to $\overline{\langle \mathbf{R}_T^2(L) \rangle}$ and $\overline{\langle \mathbf{R}_F^2(L) \rangle}$ we will compute two other quantities. First, for a polymer loop of arc-length L , we will compute the quantity [6,2]

$$C(l) = \frac{1}{d} \overline{\langle (\mathbf{R}(l) - \mathbf{R}(0))^2 \rangle} = \frac{1}{d} \overline{\left(\frac{\int d\mathbf{R} d\mathbf{R}' (\mathbf{R}' - \mathbf{R})^2 Z(\mathbf{R}, \mathbf{R}'; L-l) Z(\mathbf{R}', \mathbf{R}; l)}{\int d\mathbf{R} Z(\mathbf{R}, \mathbf{R}; L)} \right)}, \quad (1.11)$$

in the limit $L \gg l$. This is a measure of the average fluctuations of a chain segment of arc-length l . Since in this case the chain is not anchored, this quantity is in some respect similar to $\overline{\langle \mathbf{R}_F^2(L) \rangle}$. Yet another quantity of interest is

$$\overline{\langle \mathbf{R}_Q^2(L) \rangle} = \overline{\left(\frac{\int d\mathbf{R} \mathbf{R} \mathbf{R}^2 Z(\mathbf{R}, \mathbf{R}; L)}{\int d\mathbf{R} Z(\mathbf{R}, \mathbf{R}; L)} \right)}, \quad (1.12)$$

which has a more direct application to the related problem of a quantum particle in a random potential [7]. The reason for this is that the partition sum of a polymer chain can be mapped to the density matrix of a quantum particle. The mapping [7,14] is given by

$$\beta \rightarrow 1/\hbar, \quad L \rightarrow \beta\hbar. \quad (1.13)$$

Then $\rho(R, R'; \beta) = Z(R, R'; L = \beta\hbar, \beta = 1/\hbar)$ is the density matrix of a quantum particle at inverse temperature β . Note that the variable u is now interpreted as the Trotter (imaginary) time, and M as the mass of the quantum particle. Under this mapping $\overline{\langle \mathbf{R}_Q^2(L) \rangle}$ can be interpreted as the average mean squared displacement of a quantum particle in a random plus harmonic potential.

The paper is organized as follows: In Sec. II we outline the exact analytical solution for various quantities relevant to a polymer chain. In the next section we present the details of the numerical approach to the problem. In Sec. IV we compare the analytical and numerical

results and comment on the physical implications of our results. Concluding remarks are offered in Sec. V.

II. THE ANALYTICAL SOLUTION

We start with the case when one end point is fixed. The analytical calculation is based on an exact evaluation of the replicated partition sum (1.6). For the correlation function f that we are considering the replicated Hamiltonian is

$$H_n = \frac{1}{2} \int_0^L du \sum_a \left[M \left(\frac{\partial \mathbf{R}_a(u)}{\partial u} \right)^2 + \mu \mathbf{R}_a^2(u) \right] + \beta \sigma \int_0^L du \int_0^L du' \sum_{ab} (\mathbf{R}_a(u) - \mathbf{R}_b(u'))^2, \quad (2.1)$$

where $\sigma = g/2\xi^2$, and where we have dropped the constant part of the function f since it only contributes an unimportant normalization factor. After expanding the quadratic term and simplifying the double integral we get the replicated Hamiltonian

$$H_n = \frac{1}{2} \int_0^L du \sum_a \left[M \left(\frac{\partial \mathbf{R}_a(u)}{\partial u} \right)^2 + (\mu + 4n\beta\sigma L) \mathbf{R}_a^2(u) \right] - 2\beta\sigma \left(\sum_a \int_0^L du \mathbf{R}_a(u) \right)^2. \quad (2.2)$$

Now, using the Gaussian transformation

$$e^{\mathbf{Q}^2/2} = \frac{1}{(2\pi)^{d/2}} \int_{-\infty}^{\infty} d\boldsymbol{\lambda} e^{(-\boldsymbol{\lambda}^2/2 - \mathbf{Q} \cdot \boldsymbol{\lambda})} \quad (2.3)$$

and letting

$$\mathbf{Q} = 2\beta\sqrt{\sigma} \left(\sum_a \int_0^L du \mathbf{R}_a(u) \right), \quad (2.4)$$

we can write the replicated partition sum as

$$Z_n(\{\mathbf{R}_a\}, \{\mathbf{R}'_a\}; L) = \frac{1}{(2\pi)^{d/2}} \int_{-\infty}^{\infty} d\boldsymbol{\lambda} e^{-\boldsymbol{\lambda}^2/2} \prod_{a=1}^n \int_{\mathbf{R}_a(0)=\mathbf{R}_a}^{\mathbf{R}_a(L)=\mathbf{R}'_a} [d\mathbf{R}_a] e^{-\beta H_a(\boldsymbol{\lambda})}, \quad (2.5)$$

where

$$H_a(\boldsymbol{\lambda}) = \int_0^L du \left[\frac{M}{2} \left(\frac{d\mathbf{R}_a(u)}{du} \right)^2 + \frac{\mu'}{2} \mathbf{R}_a^2(u) + 2\sqrt{\sigma} \boldsymbol{\lambda} \cdot \mathbf{R}_a(u) \right], \quad (2.6)$$

and where $\mu' = \mu + 4n\beta\sigma L$. The path integrals can now be evaluated directly using well known results for quadratic Hamiltonians. The details of the calculation are given in the Appendix. Once the partition sum is known we can directly evaluate the right hand side of Eq. (1.8) by taking $n \rightarrow 0$ at the very end. The result is

$$\overline{\langle \mathbf{R}_T^2(L) \rangle} = \frac{d}{\beta} \sqrt{\frac{1}{M\mu}} \tanh\left(\sqrt{\frac{\mu}{M}} L\right) + \frac{4\sigma d}{\mu^2} \left(1 - \frac{1}{\cosh\left(\sqrt{\frac{\mu}{M}} L\right)}\right)^2, \quad (2.7)$$

We can also compute the averaged mean displacement square $\overline{\langle \mathbf{R}_T(L) \rangle^2}$ (see Appendix).

We find that

$$\overline{\langle \mathbf{R}_T(L) \rangle^2} = \frac{4\sigma d}{\mu^2} \left(1 - \frac{1}{\cosh\left(\sqrt{\frac{\mu}{M}} L\right)}\right)^2. \quad (2.8)$$

This implies that the displacement from the average is

$$\overline{\langle \mathbf{R}_T^2(L) \rangle - \langle \mathbf{R}_T(L) \rangle^2} = \frac{d}{\beta} \sqrt{\frac{1}{M\mu}} \tanh\left(\sqrt{\frac{\mu}{M}} L\right), \quad (2.9)$$

which is independent of disorder. We will discuss the physical implications of these results in a later section.

Considering now a chain that is free to move we calculate (see Appendix for details) the quantity $\overline{\langle \mathbf{R}_F^2(L) \rangle}$ using Eq. (1.9). The result is

$$\overline{\langle \mathbf{R}_F^2(L) \rangle} = \frac{2d}{\beta\sqrt{M\mu}} \frac{\sinh\left(\sqrt{\frac{\mu}{M}} L\right)}{\left(\cosh\left(\sqrt{\frac{\mu}{M}} L\right) + 1\right)}, \quad (2.10)$$

which is independent of disorder and in the limit of $\mu \rightarrow 0$ behaves like $dL/\beta M$, i.e. like a free chain.

The quantity $\overline{\langle \mathbf{R}_Q^2(L) \rangle}$ can also be computed exactly from the expression

$$\overline{\langle \mathbf{R}_Q^2(L) \rangle} = \lim_{n \rightarrow 0} \frac{\int d\mathbf{R}_1 \cdots d\mathbf{R}_n \mathbf{R}_1^2 Z_n(\{\mathbf{R}_a\}, \{\mathbf{R}_a\}; L)}{\int d\mathbf{R}_1 \cdots d\mathbf{R}_n Z_n(\{\mathbf{R}_a\}, \{\mathbf{R}_a\}; L)}. \quad (2.11)$$

Details are given in the Appendix. However, in this case it is also possible to carry out the computation in an alternative way by taking advantage of the periodic boundary conditions of the closed loop. This provides for a further check on the result and is also included for instructional purposes. Using the Fourier space variables

$$\mathbf{R}_a(\omega) = (1/\sqrt{L}) \int_0^L du \mathbf{R}_a(u) e^{-i\omega u},$$

we can write the propagator associated with βH_n as

$$\begin{aligned}\beta G_{ab}(\omega) &= \frac{\beta}{d} \langle \mathbf{R}_a(\omega) \cdot \mathbf{R}_b(-\omega) \rangle \\ &= \left\{ (M\omega^2 + \mu + 4n\beta\sigma L) \mathbf{I} - 4\beta\sigma L \delta_{\omega,0} \right\}_{ab}^{-1},\end{aligned}\quad (2.12)$$

where ω is restricted to the discrete values

$$\omega_m = \frac{2\pi}{L} m, \quad m = 0, \pm 1, \pm 2, \dots \quad (2.13)$$

After inverting the $n \times n$ matrix and taking the $n \rightarrow 0$, we find

$$\beta G_{ab}(\omega = 0) = \frac{\delta_{ab}}{\mu} + \frac{4\beta\sigma L}{\mu^2}, \quad (2.14)$$

$$\beta G_{ab}(\omega \neq 0) = \frac{\delta_{ab}}{M\omega^2 + \mu}. \quad (2.15)$$

Then, using the relation

$$\langle \mathbf{R}_a^2(L) \rangle = \frac{d}{L} \sum_{\omega} G_{aa}(\omega), \quad (2.16)$$

we find that

$$\overline{\langle \mathbf{R}_Q^2(L) \rangle} = \frac{1}{n} \sum_{a=1}^n \langle \mathbf{R}_a^2(L) \rangle = \frac{4\sigma d}{\mu^2} + \frac{d}{2\beta\sqrt{M}\mu} \coth \left(\sqrt{\frac{\mu}{M}} \frac{L}{2} \right), \quad (2.17)$$

which implies that the only effect of the disorder is to shift the zero disorder result by a constant factor. Next, we compute the quantity $\overline{\langle \mathbf{R}_Q(L) \rangle^2}$. We find that

$$\begin{aligned}\overline{\langle \mathbf{R}_Q(L) \rangle^2} &= \frac{1}{n(n-1)} \sum_{a \neq b}^n \langle \mathbf{R}_a(L) \cdot \mathbf{R}_b(L) \rangle \\ &= \frac{d}{Ln(n-1)} \sum_{a \neq b}^n \sum_{\omega} G_{ab}(\omega) = \frac{4\sigma d}{\mu^2},\end{aligned}\quad (2.18)$$

which again implies that the deviation from the average $\overline{\langle \mathbf{R}_Q^2(L) \rangle} - \langle \mathbf{R}_Q(L) \rangle^2$ is independent of disorder.

Finally, we compute the quantity $C(l)$, which was defined in Eq. (1.11). We use,

$$\begin{aligned}C(l) &= \frac{1}{nd} \sum_{a=1}^n \langle (\mathbf{R}_a(l) - \mathbf{R}_a(0))^2 \rangle \\ &= \frac{2}{nL} \sum_{a=1}^n \sum_{\omega} G_{aa}(\omega) (1 - e^{-i\omega l}) = \frac{2}{\beta L} \sum_{\omega \neq 0} \frac{1 - e^{-i\omega l}}{M\omega^2 + \mu},\end{aligned}\quad (2.19)$$

which for large L yields the expression

$$C(l) = \frac{1}{\beta\sqrt{M\mu}} \left(1 - \exp(-l\sqrt{\mu/M})\right). \quad (2.20)$$

So we find that $C(l)$ is independent of the disorder and is the same as that of a free chain.

III. NUMERICAL PROCEDURE

In order to check the validity of the analytical solution we will have to numerically compute the quenched average of certain physical properties of the polymer. This is a rather computationally intensive task because of the difficulty of evaluating the partition sum, and also because all quantities will then have to be averaged over many realizations of the random potential. In this paper we will only concentrate on the case $d = 1$. Although this does not correspond to a physical polymer ($d = 3$) we will still be able to check the validity of our analytical results for the special case $d = 1$. In the context of the quantum particle in a random potential this case corresponds to a particle in a one dimensional random potential.

We evaluate the path integral (1.3) numerically by mapping it to the associated Schrödinger equation. In dimension $d = 1$ this mapping (see Ref. [14] Eqs. (3.12)-(3.18)) is given by

$$Z(R, R'; L) = \int_{R(0)=R'}^{R(L)=R} [dR(u)] \exp(-\beta H[R(u)]) = \langle R | \exp(-\beta L \hat{H}) | R' \rangle, \quad (3.1)$$

where

$$\hat{H} = -\frac{1}{2M\beta^2} \frac{\partial^2}{\partial \hat{R}^2} + \frac{\mu}{2} \hat{R}^2 + V(\hat{R}). \quad (3.2)$$

We compute the matrix element by expanding it in terms of the energy eigenstates of \hat{H}

$$\langle R | \exp(-\beta L \hat{H}) | R' \rangle = \sum_n \exp(-\beta L E_n) \Phi_n(R)^* \Phi_n(R'). \quad (3.3)$$

In order to compute the eigenvalues and eigenvectors numerically we solve the Schrödinger equation on a one dimensional lattice of N sites [15]. The lattice Hamiltonian is then an

$N \times N$ matrix with matrix elements given by

$$H_{ij} = -\frac{1}{2M\beta^2\Delta^2} (\delta_{i,j+1} + \delta_{i+1,j}) + \left(\frac{\mu}{2}\Delta^2(i - N/2)^2 + V(i)\right) \delta_{i,j} \quad (3.4)$$

where the lattice spacing is $\Delta = S/N$, and where S is the system size. Since we are interested in the continuum limit Δ will be kept small. Note that the index i corresponds to the position $R_i = \Delta i$. The eigenvalues and eigenvectors can now be found directly by diagonalizing the matrix using a standard numerical routine [15]. Once these are known we can construct the partition sum at any value of L using Eq. (3.3).

The random potential $V(R)$ is generated by first generating a Gaussian correlated random potential $V_\xi(R)$ that satisfies

$$\langle V_\xi(R)V_\xi(R') \rangle \propto \exp(-(R - R')^2/\xi^2). \quad (3.5)$$

Since we are making a lattice approximation we need a sequence of N numbers $\{V_\xi(i)\}_{i=1,\dots,N}$ that obey $\langle V_\xi(i)V_\xi(i+l) \rangle \propto G(l)$, where in this case $G(l) = \exp(-\Delta^2 l^2/\xi^2)$. These numbers will then be placed on the N lattice sites in the given order. To generate such numbers we use a method described in reference [16]. The procedure is to first generate a sequence of N uncorrelated random numbers $\{U(i)\}$ with a Gaussian distribution. These numbers are then fast Fourier transformed, using a standard numerical routine [15], to yield the sequence $\{\tilde{U}(i)\}$. Next, we calculate the N numbers defined by $\tilde{W}(i) = \sqrt{\tilde{G}(i)}\tilde{U}(i)$, where $\tilde{G}(i)$ is defined as the Fourier transform of the correlation function $G(i)$. Finally, taking the inverse Fourier transform of the sequence $\{\tilde{W}(i)\}$, yields $\{W(i)\}$, the sequence with the desired correlation function $G(i)$. Now, in order to generate quadratic correlations we choose ξ such that the Gaussian correlation function is well approximated by its leading quadratic term over the range of the system size. The approximate condition for this to hold is that $\xi/S \gtrsim 1/\sqrt{2}$. In this way we generate a well defined set of random numbers which obey approximately the correlation function given in Eq. (1.10).

In Fig. 1 we plot a correlation function that is generated by the above method. On the same graph we plot the corresponding quadratic approximation. Notice that in this case when $|R - S/2| \sim 10$ the quadratic approximation begins to deviate from the generated

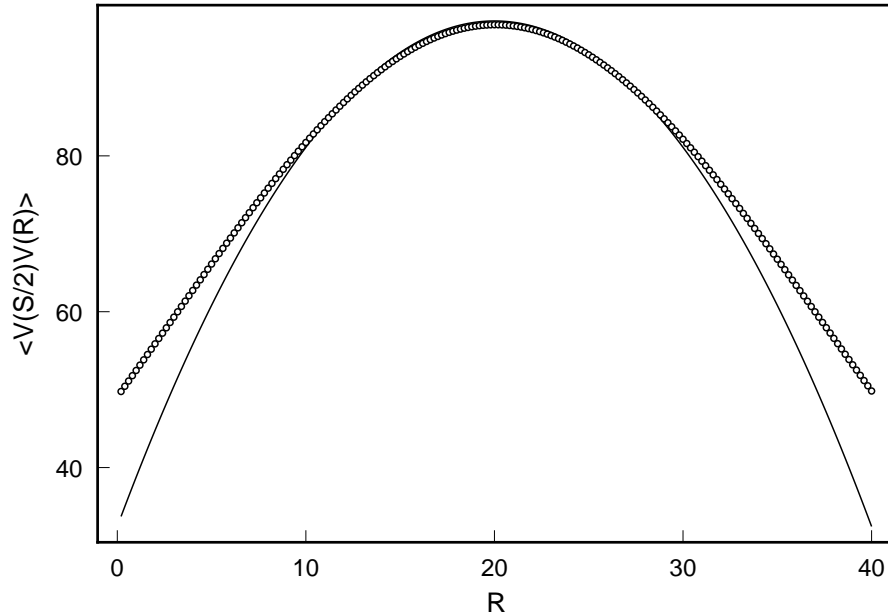


FIG. 1. Plot of $\langle V(S/2)V(R) \rangle$ versus R . The circles are generated by averaging over 10,000 samples. The solid line is a plot of the quadratic approximation to the correlation function given by Eq. (3.5). The parameters are $\xi = 10\sqrt{6}$, $S = 40$, $N=200$.

correlation function. This discrepancy turns out to be unimportant as long the quantities that are numerically computed (such as end to end distance) do not exceed this range of validity. In order to reduce errors due to the finite size of the lattice we found it useful to take our sample of random numbers from a set which was about five times N . In all cases we tested the reliability of the samples by directly computing the correlation function and comparing to the analytical expression for the correlation function given by Eq. (3.5).

IV. RESULTS AND DISCUSSION

We discretized the Schrödinger equation on a lattice of size $N = 200$. Once the eigenvalues and eigenvectors are known then we can approximate, for instance the mean squared displacement, for each random sample. We then average over the samples to get an approximation to the quenched average. For simplicity we set $M = 1/2$ and $\beta = 1$ for all cases.

In Fig. 2 we graph the mean squared displacement with one endpoint fixed as a function

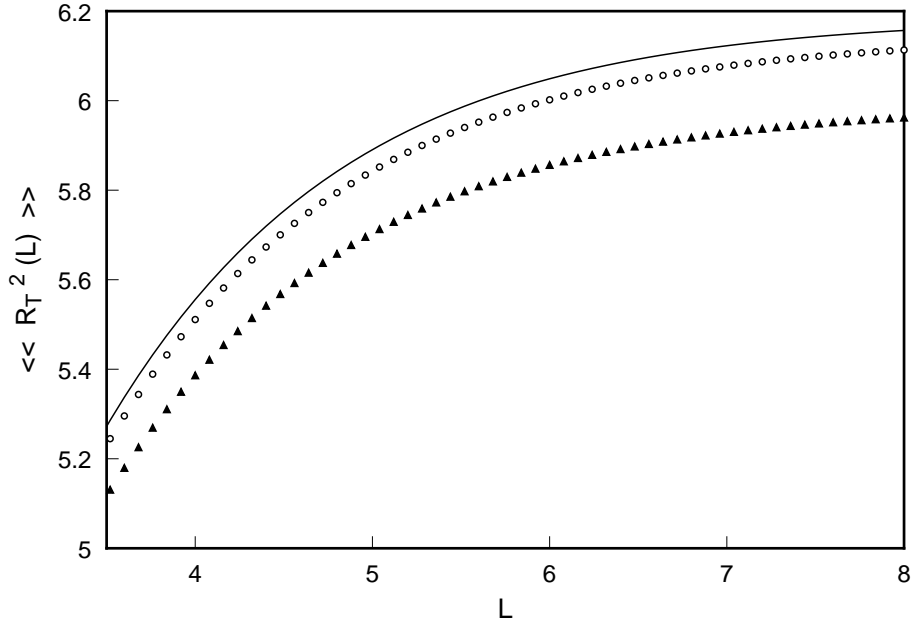


FIG. 2. Plot of $\langle\langle R_T^2(L) \rangle\rangle$ as a function of L . The parameters are $\mu = 0.3$, $\sigma = 0.0811$, $\Delta = 0.2$, $\xi = 10\sqrt{6}$. The solid line corresponds to the analytical solution given in Eq. (2.7). The triangles are generated by averaging over 1000 samples and the circles represent averaging over 10,000 samples.

of L . We do this for two different number of samples in order to check convergence towards the corresponding analytical solution. Note that in the labels of the plots the average over the disorder is denoted by a second set of brackets rather than an overbar. In Fig. 3 we graph $\langle\langle R_T(L) \rangle\rangle^2$ as a function of L . We use the same parameters as in Fig. 2. It is clear from the graphs that the numerical results are consistent with the exact curve. As the number of the samples is increased the numerical curves get closer to the analytical solution. In Fig. 4 we plot $\overline{\langle R_F^2(L) \rangle}$ vs. L . This quantity is computed numerically using the expression given in Eq. (1.5). We found that the numerical results were extremely close to the analytical prediction after averaging over only 200 samples.

We now turn our attention to the quantity $\overline{\langle R_Q^2(L) \rangle}$, which was discussed in the introduction. In Fig. 5. we graph $\overline{\langle R_Q^2(L) \rangle}$ vs. L . In order to visualize the predicted shift in Eq. (2.17) we include the exact solution of the zero disorder case. We use the same parameters as the previous figures. Again, we find close agreement between the computational results and the analytical solution. The shift due to the disorder is clearly evident and is

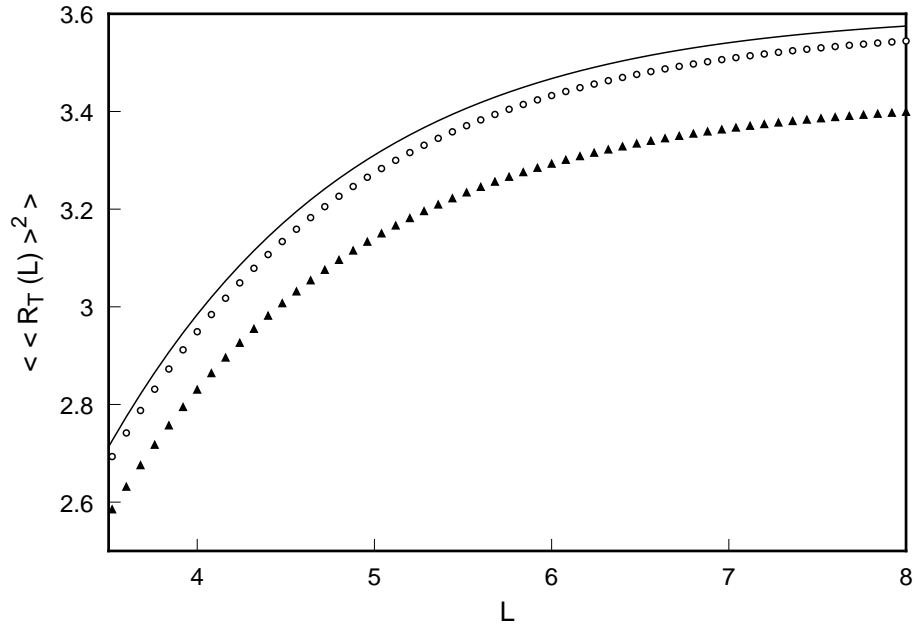


FIG. 3. Plot of $\overline{\langle R_T(L) \rangle^2}$ as a function of L . The solid line is a graph of the analytical solution in Eq. (2.8). The triangles are generated by averaging over 1000 samples and the circles represent averaging over 10,000 samples.

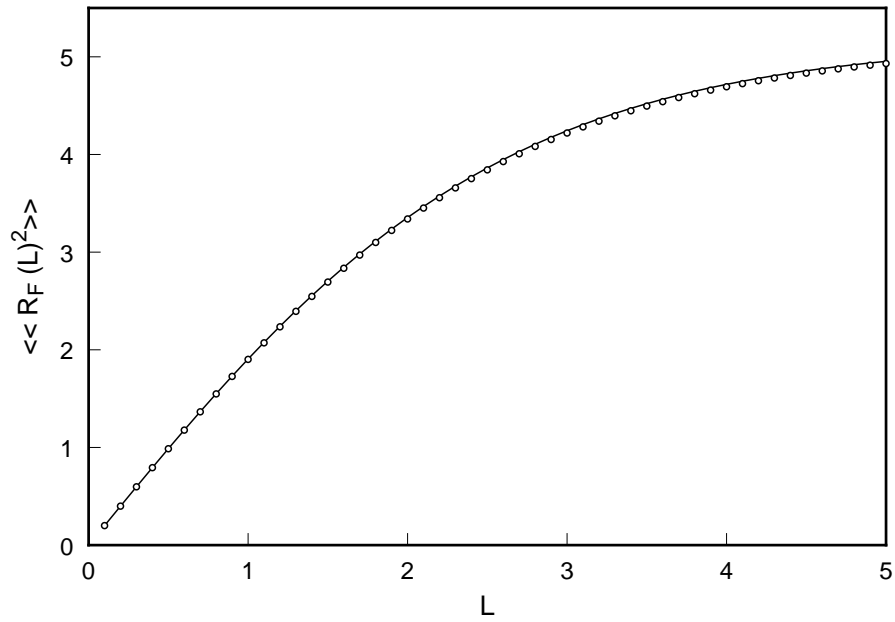


FIG. 4. Plot of $\overline{\langle R_F(L) \rangle^2}$ as a function of L . The solid line corresponds to the analytical solution given in Eq. (2.10). The circles are generated by averaging over 200 samples. All the parameters are the same as in Fig 2.

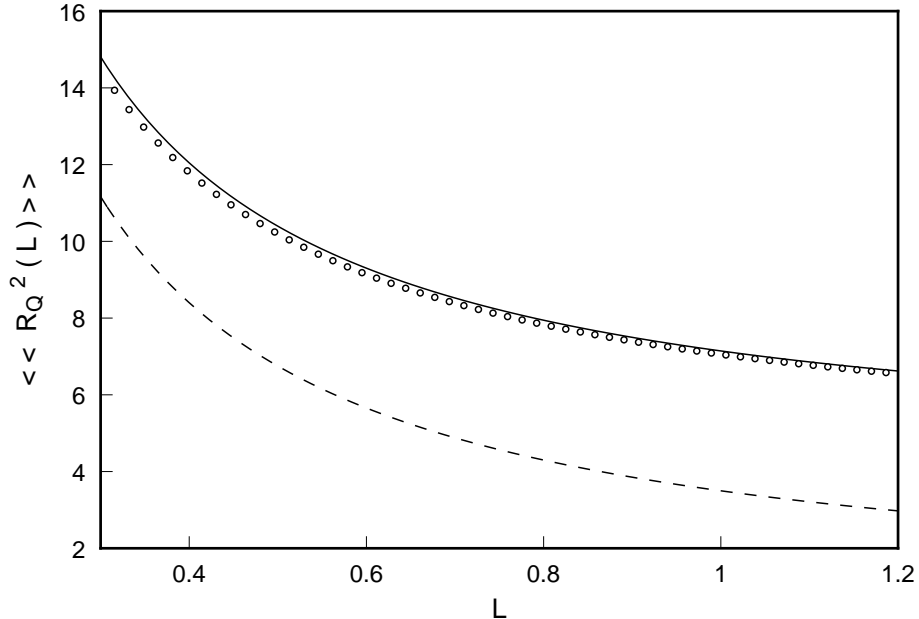


FIG. 5. Plot of $\overline{\langle R_Q^2(L) \rangle}$ vs. L . The solid line is the analytical solution given in Eq. (2.17). The circles are generated by averaging over 8000 samples. The dashed line is the analytical solution for zero disorder ($\sigma = 0$).

very close to the predicted value. In Fig. 6 we plot $\overline{\langle R_Q(L) \rangle^2}$ vs. L and compare with a plot of the analytical solution in Eq. (2.18). For small L there appears to be a discrepancy between the data and the analytical solution, whereas for larger L the two curves are very close. This is due to the fact that the random potential is generated on a grid with grid size of 0.2. Thus for L shorter than 0.2 the particle can not see the random potential and $\overline{\langle R_Q(L) \rangle^2}$ vs. L should average to zero. Indeed the significant deviation occurs on this length scale.

Finally, we turn our attention to the quantity $C(l)$. It was evaluated numerically from the expression given in Eq. (1.11). In Fig. 7 we plot $C(l)$ vs. l with L large and fixed.

It is clear from the graphs that the numerical solutions are consistent with the exact analytical solution. As expected, as the number of samples is increased the numerical results get closer and closer to the exact curve. Based on these results we can safely conclude that the replica calculation is indeed correct and does describe the averaged properties of the polymer.

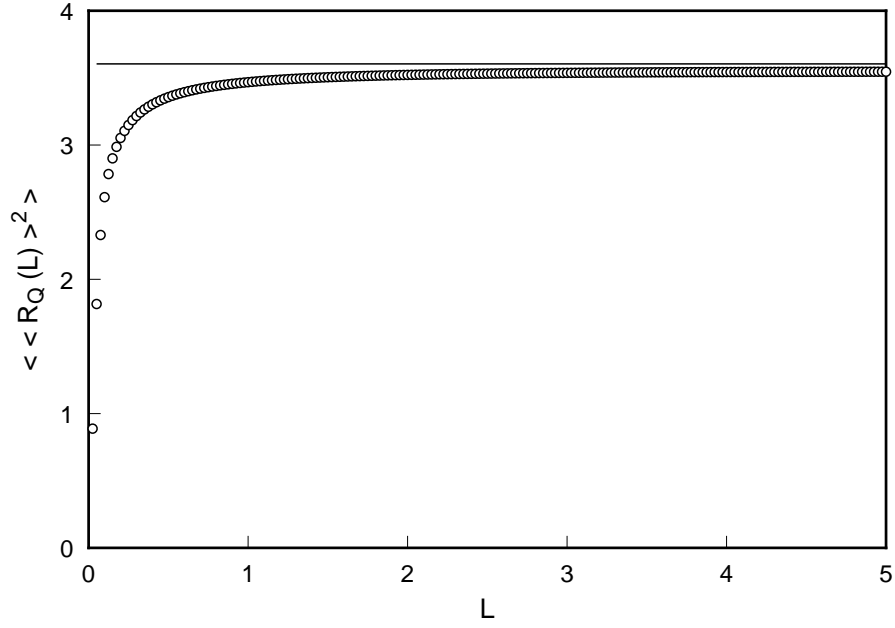


FIG. 6. Plot of $\overline{\langle R_Q(L) \rangle^2}$ vs. L . The solid line is the analytical solution given in Eq. (2.18). The circles are generated by averaging over 8000 samples.

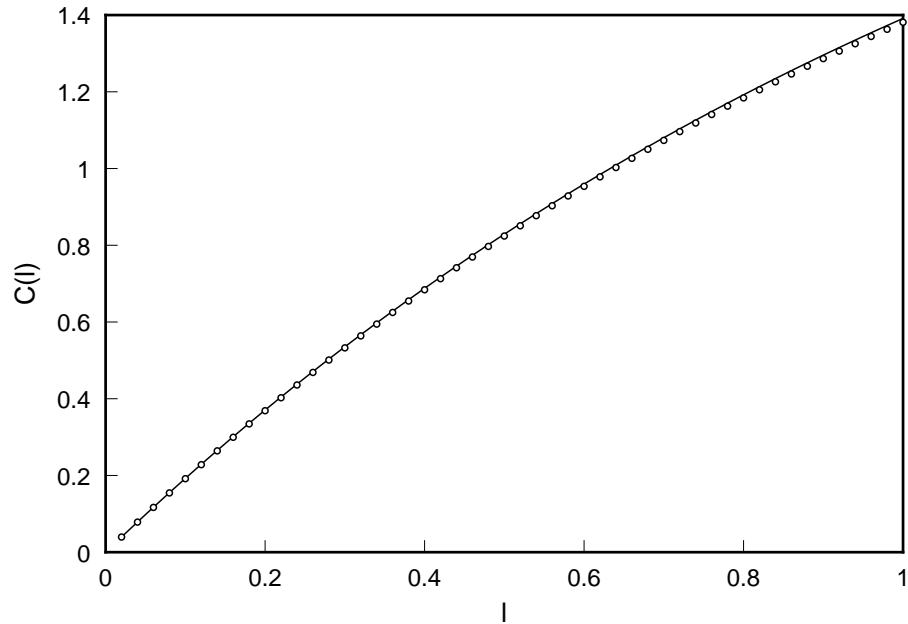


FIG. 7. Plot of $C(l)$ vs. l , with $L = 10$. The solid line is the analytical solution given by Eq. (2.20). The circles are generated by averaging over 250 samples. All parameters are the same as the previous graphs.

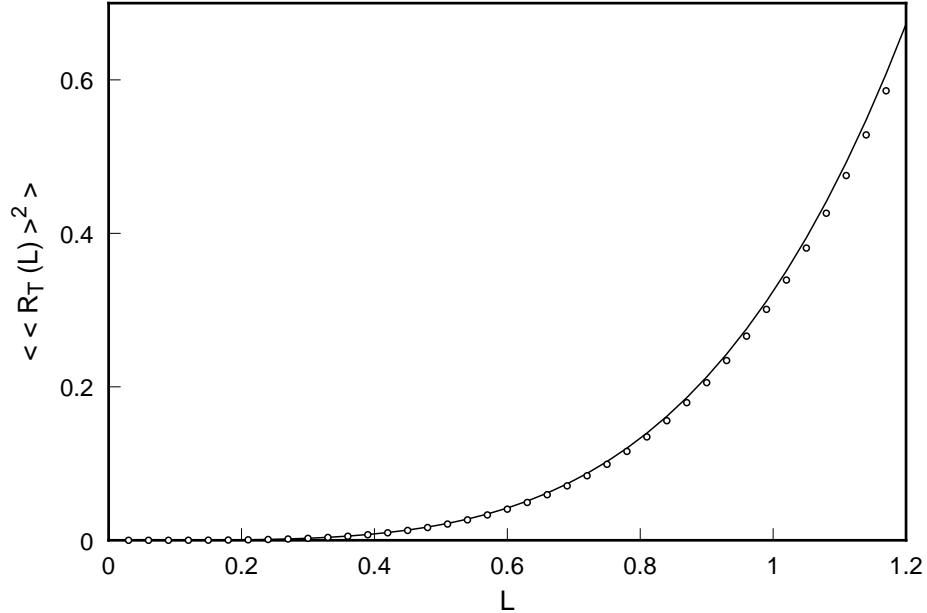


FIG. 8. Plot of $\overline{\langle R_T(L) \rangle^2}$ vs. L . The solid line is the analytical solution given in Eq. (4.2). The circles are generated by averaging over 1000 samples. We take $\mu = 0.001$, and all other parameters are the same as in Fig. 2.

It is interesting to study the infinite volume limit $\mu \rightarrow 0$. Here, the polymer does not see the confining harmonic potential and its properties are determined only by the random potential. Taking the $\mu \rightarrow 0$ limit the exact expressions simplify to

$$\overline{\langle \mathbf{R}_T^2(L) \rangle} = \frac{d}{\beta M} L + \frac{d\sigma}{M^2} L^4, \quad (4.1)$$

$$\overline{\langle R_T^2(L) \rangle^2} = \frac{d\sigma}{M^2} L^4. \quad (4.2)$$

Notice that in the no disorder case ($\sigma = 0$) the later quantity is zero, but once the disorder is turned on it scales like L^4 with a coefficient that is independent of temperature. Also, Eq. (4.1) indicates that for small L the polymer wanders diffusively but for larger L it wanders much faster than diffusion. In Fig. 8 we plot $\overline{\langle R_T(L) \rangle^2}$ vs. L when μ is chosen to be very small. On the same graph we plot Eq. (4.2). In Fig. 9 we plot $\overline{\langle R_T^2(L) \rangle - \langle R_T(L) \rangle^2}$ vs. L . On the same graph we include the analytical prediction. It is clear that the numerical results agree well with the analytical predictions. Also, from Eq. (2.17) we see that the quantity $\overline{\langle \mathbf{R}_Q^2(L) \rangle}$ diverges as $\mu \rightarrow 0$. This implies that the boundary conditions on the

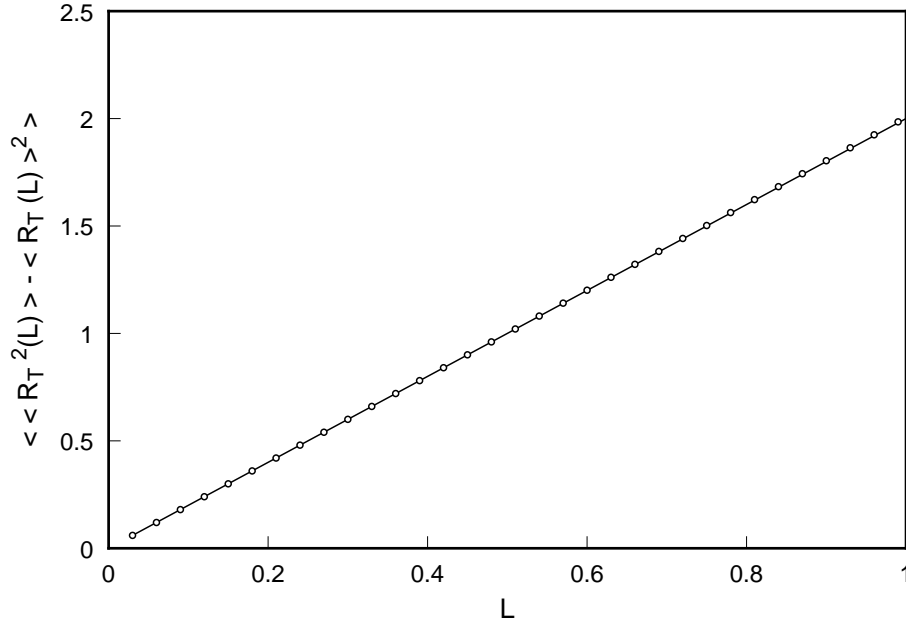


FIG. 9. Plot of $\overline{\langle R_T^2(L) \rangle} - \langle R_T(L) \rangle^2$ vs. L . The solid line is the analytical solution given by subtracting Eq. (4.2) from Eq. (4.1). The circles generated by averaging over 1000 samples. We take $\mu = 0.001$, and all other parameters are the same as in Fig. 2.

chain are crucial in determining which quantities are well defined in the infinite volume limit.

The physical consequences of our results are surprising and may seem counter intuitive at first glance. The very long range correlations of the random potential lead to a very fast wandering of the free end of a tethered chain. However, the deviation from the average position $\overline{\langle \mathbf{R}_T^2(L) \rangle} - \langle \mathbf{R}_T(L) \rangle^2$ does not depend on the random potential. Also, if both ends are free to move then the end to end distance $\overline{\langle \mathbf{R}_F^2(L) \rangle}$ behaves as if there is no random potential. This behavior can make more sense if we study the nature of the random potential samples that satisfy the quadratic correlation. We find that the typical random potential (see Fig. 10) is smooth and slowly varying on short scales but contains peaks and valleys on scales close to the system size. So as L is increased the polymer has a greater tendency to be found in the deepest potential well in the sample, which, for large sample sizes, is on average located very far from the fixed end of the polymer. So for the case when one end is fixed we expect the end to end distance to grow very fast with L , as the bulk (center

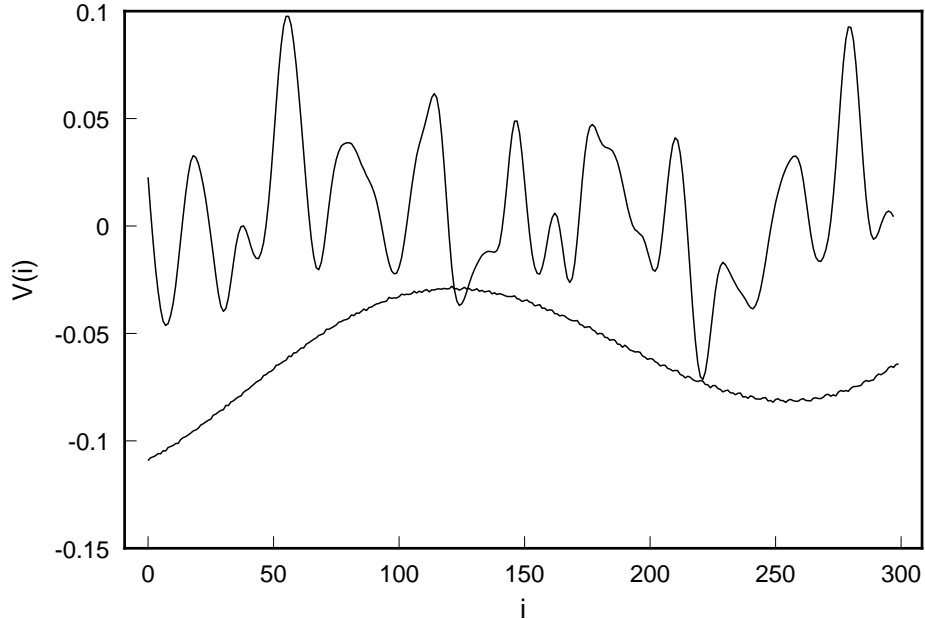


FIG. 10. The lower curve represents a typical random potential with long range quadratic correlations ($\xi = 10\sqrt{6}$). For comparison the upper curve represents a random potential with a shorter correlation range ($\xi = 1$).

of mass) of the polymer moves far away from the fixed end. This behavior is the same as in the case of short range correlations [3], where the polymer will typically form a tadpole conformation with the tail tethered to the origin and the head far away in some region of low potential. On the other hand, when both ends are free the entire polymer will simply curl up in the region of low potential and the end to end distance should depend only on the local behavior of the random potential. Now, since the potential samples are smooth and slowly varying on short scales we do not expect the disorder to have much of an effect on the local behavior of the polymer. What is very interesting though is the fact that the chain that is free to move behaves as if the random potential has no effect at all. Similarly, the fluctuations around the average position in the case when one end is fixed turn out to be totally independent of disorder. This is expected to be a special feature of the quadratically correlated random potential, and is not likely to hold in the general case of long range correlations. See discussion below about the crossover to shorter ranged correlations of the disorder.

It is useful to compare our results with those for directed polymers. Here, the arc-length u corresponds to the distance along the directed axis which is a fixed direction in real space, and the vector $\mathbf{R}(u)$ is the position of the directed line in the transverse hyper-plane. In that case the random potential is usually taken to depend on u and satisfy

$$\langle V(\mathbf{R}, u)V(\mathbf{R}', u') \rangle = \delta(u - u')f((\mathbf{R} - \mathbf{R}')^2), \quad (4.3)$$

i. e. the random potential is taken to be uncorrelated along the directed axis, unlike the situation described in Eqs. (1.1,1.2) where the random potential is independent of u . Parisi has shown [10] that if f is quadratic, then the mean squared displacement of one end of the directed polymer satisfies $\overline{\langle \mathbf{R}_T^2(L) \rangle} \propto L^3$. This is to be compared with the L^4 dependence that we have found for the case when the random potential is independent of u .

To explain the different scaling we employ a Flory-type argument similar to the argument used in [11] for directed polymers. Allowing for a rescaling of the arc-length variable u by a scale ℓ , i.e. $u \rightarrow \ell u$ and the position variables $\mathbf{R}(u) \rightarrow \ell^\zeta \mathbf{R}(\ell u)$ we see that the random potential which satisfies Eq. (1.2) with a correlation function behaving in general like

$$f((\mathbf{R} - \mathbf{R}')^2) \sim \text{const.} - \frac{2\sigma}{1 - \alpha} (\mathbf{R} - \mathbf{R}')^{2(1-\alpha)}, \quad (4.4)$$

scales like ℓ^λ with

$$2\lambda = \zeta 2(1 - \alpha) \quad (4.5)$$

The difference with directed polymers is that in that case one has to subtract a 1 from the right hand side of Eq. (4.5) because of the delta function in Eq (4.3). Now in a Flory argument one assumes that the two terms in the hamiltonian given in Eq. (1.1) scale the same way (here we consider only the case of $\mu = 0$, since $\mu \neq 0$ breaks scale invariance). Since the 'kinetic' energy term scales like $\ell^{2\zeta-2}$, and this should be equal to ℓ^λ , we see that

$$\zeta = \frac{2}{1 + \alpha}. \quad (4.6)$$

Thus $\overline{\langle \mathbf{R}_T^2(L) \rangle} \sim L^{4/(1+\alpha)}$ as opposed to $L^{3/(1+\alpha)}$ for directed polymers. In the quadratic case $\alpha = 0$, and we get the L^4 behavior we were looking for. Notice that we derived here

a prediction for the behavior of $\overline{\langle \mathbf{R}_T^2(L) \rangle}$ for the case of long ranged correlations of the disorder which are not quadratic but are characterized by a power law determined by the value of α . Thus the power of L will decrease for shorter ranged correlations than quadratic. It is interesting to assess the accuracy of the Flory argument in practice. In the function $\overline{\langle \mathbf{R}_T^2(L) \rangle - \langle \mathbf{R}_T(L) \rangle^2}$ or in $\overline{\langle \mathbf{R}_F^2(L) \rangle}$ the leading power of L cancels out and one is left with a subleading L^1 behavior (for quadratic correlations).

Within this toy model it is interesting to compare the differences between the annealed and the quenched averages. The annealed average applies when the obstacles in the medium are randomly placed and mobile. In this case the replica trick is not necessary and the random potential can be averaged directly. Alternatively one can use the results obtained with Z_n but instead of taking n to 0, substituting $n = 1$. We easily find that

$$\overline{\langle \mathbf{R}_T^2(L) \rangle} = \frac{\int d\mathbf{R} \mathbf{R}^2 \overline{Z(\mathbf{0}, \mathbf{R}, L)}}{\int d\mathbf{R} \overline{Z(\mathbf{0}, \mathbf{R}, L)}} \sim \frac{1}{\sqrt{\sigma L}}, \quad (4.7)$$

when L is large, and where we have taken the $\mu \rightarrow 0$ limit. So in an annealed medium with long range quadratic correlations a very long polymer chain will collapse around the tethered end. Similarly, we find that $\overline{\langle \mathbf{R}_F^2(L) \rangle} \sim 1/\sqrt{\sigma L}$, and so if both ends are free then the polymer will collapse in the same way. This behavior is in stark contrast to the quenched case where the effects of the random medium is quite different.

For the case of short ranged correlations and a chain that is free to move one usually argues [3] that the annealed and quenched averages coincide in the infinite volume limit. This is due to the fact that the system can be divided into subregions, much larger than the chain, each containing a different realization of the potential. The moving chain can sample all of these and find a realization very similar to the one it induces around itself in the annealed case. But this argument does not apply to the case of long ranged correlations of the random potential, with the correlation length larger than the system size, since such a division to subregions will not yield independent realizations.

It will be interesting to investigate how the physical properties that we have found change as we move towards the regime of short range correlations. In our model we can control the correlation length by varying the parameter ξ in Eq. (3.5) i.e. in the Gaussian form.

For small ξ the correlation is certainly not quadratic, and it approaches a δ -function in the limit $\xi \rightarrow 0$. For arbitrary ξ we expect that the average mean displacement squared in $d = 1$ will scale as $\overline{\langle R_T(L) \rangle^2} \propto L^{\gamma(\xi)}$. Numerically, we can estimate the exponent $\gamma(\xi)$ by performing a linear fit to the plot of $\log \overline{\langle R_T(L) \rangle^2}$ vs. $\log L$ and measuring the slope. For short range correlations we found that the numerical method described in Sec. III was unreliable. The reason for this is that the sum over energy eigenfunctions in Eq. (3.3) is unstable since a typical overlap $\Phi_n(R)^* \Phi_n(R')$ (for short range correlations) is a number on the order of 10^{-15} . However, we were able to evaluate Eq. (3.3) accurately for all ξ by solving the Schrödinger equation on a lattice using a fourth order Runge-Kutta algorithm with a very small time step ($t \sim 10^{-4}$). We found that for large L the quantity $\overline{\langle R_T(L) \rangle^2}$ saturates at a constant value due to the finite size of the system, and so we do not expect a power law scaling for large L . However, for L sufficiently small (before the onset of saturation) the mean displacement squared does obey a power law and a linear fit on a log-log plot was excellent for all ξ .

In Fig. 11 we plot γ vs. $1/\xi^2$ for a range of ξ . For each point we averaged over 8000 samples on a lattice of size $N = 300$, and in all cases the strength of the random potential is taken to be large ($g \gg 1$). We can see from the plot that γ falls from 4, in the case of very long range correlations, to about 2.5 for very short range correlations. The case of delta correlated random potentials has been studied by Nattermann [4] using Flory arguments. Nattermann finds that for strong disorder ($g \gg 1$) the mean squared displacement behaves like $\overline{\langle R_T(L)^2 \rangle} \propto L^2 \sqrt{g} (\ln(L))^{-3/2}$ in $d = 1$. It is clear from Nattermann's arguments that $\overline{\langle R_T(L)^2 \rangle} \sim \overline{\langle R_T(L) \rangle^2}$, and so it is safe to compare our numerical results with his analytical expression. So while we find a scaling that is slightly faster than ballistic ($\sim L^{2.5}$), Nattermann finds a weakly subballistic behavior ($\sim L^2 \ln(L)^{(-3/2)}$). Nevertheless, it is comforting to see that both results are fairly close to a ballistic scaling ($\sim L^2$).

We now turn our attention to the chain that is free to move. Here, we find that for short range correlations ($\xi \lesssim \sqrt{5}$) the end-to-end distance rises linearly for small L and saturates at a constant value for large L . This saturation is not due to the finite size of the system

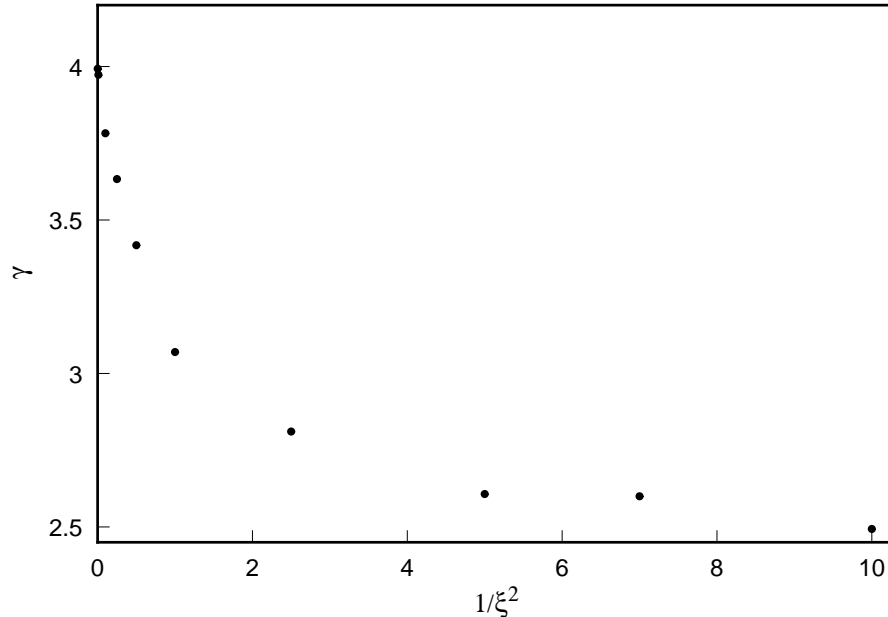


FIG. 11. Plot of γ vs. $1/\xi^2$.

since it occurs at a value of L far less than the length at which a free chain would saturate. Typically, for $L \gtrsim 1$ we find that $\overline{\langle R_F^2(L) \rangle} \propto L^0$ as compared to $\overline{\langle R_F^2(L) \rangle} \propto L$ when the correlations are long range and quadratic. In order to quantify this crossover between the long and short range behavior we assume that the scaling relation $\overline{\langle R_F^2(L) \rangle} \propto L^{\delta(\xi)}$ holds for $L \gtrsim 1$. Again we can estimate the exponent $\delta(\xi)$ by measuring the slope of the line in a linear fit of $\log \overline{\langle R_F^2(L) \rangle}$ vs. $\log L$.

In Fig. 12 we plot δ vs. $1/\xi^2$ for a range of ξ . We computed the end-to-end distance for L in the range $5 < L < 10$. For each point we averaged over 1000 samples on a lattice of size $N = 200$, and in all cases the strength of the random potential is taken to be large ($g \gg 1$). We can see from the graph that as the correlation range is decreased δ falls rapidly from about 1 to a value close to zero. This implies that the behavior of $\overline{\langle R_F^2(L) \rangle}$ is very strongly dependent on the correlation range. These results are consistent with the Flory arguments in Ref. [3,4] where it is predicted that a long polymer in a delta correlated random potential will have fixed size i.e. $R^2 \sim L^0$ in a sample of finite volume, and with the variational results of Ref. [6] (see also [2,5]).

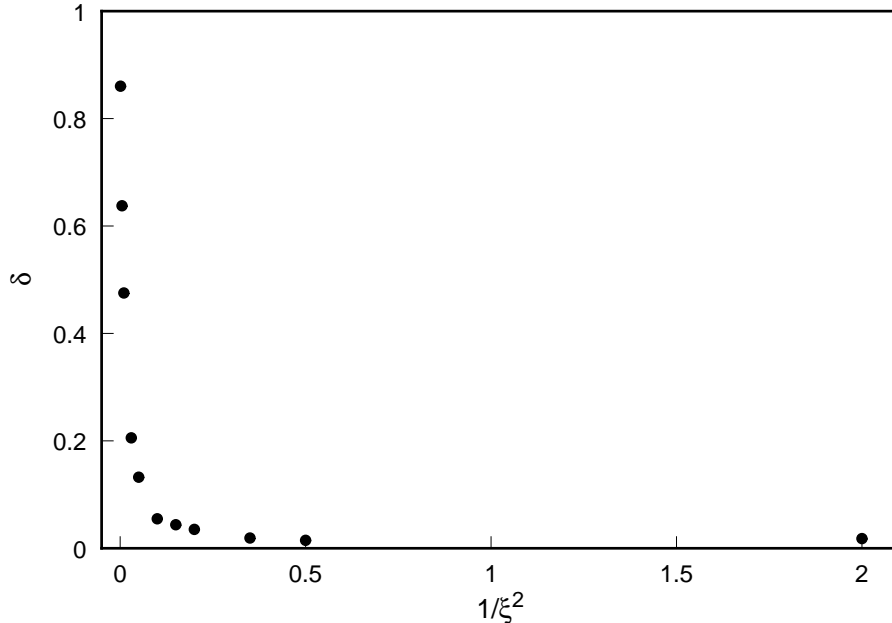


FIG. 12. Plot of δ vs. $1/\xi^2$.

V. CONCLUDING REMARKS

In this paper we presented a model of a polymer chain in a quenched random media which was exactly solvable using the replica method. The analytical results were subsequently found to be in close agreement with a numerical solution in $d = 1$. Based on these results we can safely conclude that the replica method is accurate in describing the averaged properties of the polymer. The physical picture that emerged was interesting and somewhat surprising. We found that a quadratically correlated disorder has a major effect on the size of a polymer with one end fixed, but has no effect on the size of a chain that is free to move and find an optimal position. We also found that the quenched and annealed cases are rather different: In the annealed case a long chain collapses to a point.

Overall, we have learned that chain properties depend strongly on the correlation range of the random media. However, there are still some open problems. For instance, it would be very useful to have an analytical derivation of the results depicted in Figs. 11,12. Also, it may be fruitful to investigate various non-equilibrium properties of polymer chains in long range correlated random media, such as transport properties and chain dynamics. We hope

that our results for the simple case of quadratic correlations will be a useful starting point for a more detailed analysis of these problems.

ACKNOWLEDGMENTS

Y.Y.G. acknowledges support from the US Department of Energy (DOE), grant No. DE-G02-98ER45686.

APPENDIX:

Here we show some of the intermediate steps that lead to Eq. (2.7). We first write the replicated partition sum as

$$Z_n(\{\mathbf{R}_a\}, \{\mathbf{R}'_a\}; L) = \frac{1}{(2\pi)^{d/2}} \int d\boldsymbol{\lambda} e^{-\boldsymbol{\lambda}^2/2} Z(\{\mathbf{R}_a\}, \{\mathbf{R}'_a\}; L, \boldsymbol{\lambda}), \quad (\text{A1})$$

where

$$Z(\{\mathbf{R}_a\}, \{\mathbf{R}'_a\}; L, \boldsymbol{\lambda}) = \prod_{a=1}^n \int_{\mathbf{R}_a(0)=\mathbf{R}_a}^{\mathbf{R}_a(L)=\mathbf{R}'_a} [d\mathbf{R}_a] e^{-\beta H_a(\boldsymbol{\lambda})}. \quad (\text{A2})$$

After performing the path integrals using equations (3.39 – 3.41) in [14], we get

$$Z(\{\mathbf{R}_a\}, \{\mathbf{R}'_a\}; L, \boldsymbol{\lambda}) = N_0 e^{-\beta\Phi}, \quad (\text{A3})$$

where

$$\Phi = A \left(\sum \mathbf{R}_a^2 + \sum \mathbf{R}'_a{}^2 \right) + B \left(\sum \mathbf{R}_a + \sum \mathbf{R}'_a \right) \cdot \mathbf{a} + 2C \sum \mathbf{R}_a \cdot \mathbf{R}'_a + nDa^2, \quad (\text{A4})$$

with

$$A = \frac{1}{2} \sqrt{\mu' M} \coth \left(L \sqrt{\mu' / M} \right) \quad (\text{A5})$$

$$B = \sqrt{\mu' M} \left[\cosh \left(L \sqrt{\mu' / M} \right) - 1 \right] \left[\sinh \left(L \sqrt{\mu' / M} \right) \right]^{-1} \quad (\text{A6})$$

$$C = -\frac{1}{2} \sqrt{\mu' M} \left[\sinh \left(L \sqrt{\mu' / M} \right) \right]^{-1} \quad (\text{A7})$$

$$D = B - L\mu'/2, \quad (\text{A8})$$

$$\mathbf{a} = \frac{2}{\mu'} \sqrt{\sigma} \boldsymbol{\lambda}. \quad (\text{A9})$$

The exact form of the normalization N_0 is unimportant as it will cancel out later. The next step is to perform the Gaussian integrals over the $\boldsymbol{\lambda}$ variables in Eq. (A1). This yields

$$Z_n(\{\mathbf{R}_a\}, \{\mathbf{R}'_a\}; L) = N_1 \exp \left\{ -U \left(\sum \mathbf{R}_a^2 + \sum \mathbf{R}'_a{}^2 \right) - V \left(\sum \mathbf{R}_a + \sum \mathbf{R}'_a \right)^2 - 2W \sum \mathbf{R}_a \cdot \mathbf{R}'_a \right\}, \quad (\text{A10})$$

with

$$U = \beta A \quad (\text{A11})$$

$$V = -\frac{2\sigma\beta^2 B^2}{\mu'^2 + 8\beta\sigma n D} \quad (\text{A12})$$

$$W = \beta C. \quad (\text{A13})$$

Now, for arbitrary n we can write

$$\begin{aligned} \langle \mathbf{R}_1^2(L) \rangle &= \frac{\int d\mathbf{R}_1 \cdots d\mathbf{R}_n \mathbf{R}_1^2 Z_n(\{\mathbf{0}\}, \{\mathbf{R}_a\}; L)}{\int d\mathbf{R}_1 \cdots d\mathbf{R}_n Z_n(\{\mathbf{0}\}, \{\mathbf{R}_a\}; L)} \\ &= -\frac{1}{n} \frac{d}{dU} \ln \int d\mathbf{R}_1 \cdots d\mathbf{R}_n Z_n(\{\mathbf{0}\}, \{\mathbf{R}_a\}; L) \\ &= -\frac{1}{n} \frac{d}{dU} \ln \left[\frac{\pi^n}{U^{n-1}(U + nV)} \right] \\ &= \frac{d}{2} \left(\frac{1}{U} - \frac{V}{U(U + nV)} \right). \end{aligned} \quad (\text{A14})$$

We have used the fact that the eigenvalues of the matrix associated with the quadratic form in Eq. (A10) are U with multiplicity $n - 1$ and $U + nV$ with multiplicity 1, and the determinant is the product of the eigenvalues. The $n \rightarrow 0$ can now be safely taken to yield

$$\overline{\langle \mathbf{R}_T^2(L) \rangle} = \lim_{n \rightarrow 0} \langle \mathbf{R}_1^2 \rangle = \frac{d}{2\beta A} + \frac{\sigma d}{\mu^2} \left(\frac{B}{A} \right)^2. \quad (\text{A15})$$

which simplifies to yield Eq. (2.7).

To calculate $\overline{\langle \mathbf{R}_T(L) \rangle^2}$ we use

$$\begin{aligned} \overline{\langle \mathbf{R}_T(L) \rangle^2} &= \frac{\int d\mathbf{R}_1 \cdots d\mathbf{R}_n \mathbf{R}_1 \cdot \mathbf{R}_2 Z_n(\{\mathbf{0}\}, \{\mathbf{R}_a\}; L)}{\int d\mathbf{R}_1 \cdots d\mathbf{R}_n Z_n(\{\mathbf{0}\}, \{\mathbf{R}_a\}; L)} \\ &= \frac{1}{n(n-1)} \left(\frac{d}{dU} - \frac{d}{dV} \right) \ln \int d\mathbf{R}_1 \cdots d\mathbf{R}_n Z_n(\{\mathbf{0}\}, \{\mathbf{R}_a\}; L) \\ &= \frac{1}{n(n-1)} \frac{d}{2} \left(\frac{d}{dU} - \frac{d}{dV} \right) \ln \left[\frac{\pi^n}{U^{n-1}(U + nV)} \right] \\ &= -\frac{d}{2} \left(\frac{V}{U(U + nV)} \right). \end{aligned} \quad (\text{A16})$$

Next, we show how to calculate $\overline{\langle \mathbf{R}_F^2(L) \rangle}$.

$$\begin{aligned} \overline{\langle \mathbf{R}_F^2(L) \rangle} &= \frac{\int \prod d\mathbf{R}_a \prod d\mathbf{R}'_a (\mathbf{R}_1 - \mathbf{R}'_1)^2 Z_n(\{\mathbf{R}_a\}, \{\mathbf{R}'_a\}; L)}{\int \prod d\mathbf{R}_a \prod d\mathbf{R}'_a Z_n(\{\mathbf{R}_a\}, \{\mathbf{R}'_a\}; L)} \\ &= \frac{1}{n} \left(\frac{d}{dU} - \frac{d}{dW} \right) \ln \int \prod d\mathbf{R}_a \prod d\mathbf{R}'_a Z_n(\{\mathbf{R}_a\}, \{\mathbf{R}'_a\}; L) \\ &= \frac{1}{n} \frac{d}{2} \left(\frac{d}{dU} - \frac{d}{dW} \right) \ln \left[\frac{\pi^{2n}}{(U + W)^{n-1} (U - W)^n (U + W + 2nV)} \right] \\ &= \frac{d}{U - W} = \frac{d}{\beta(A - C)}, \end{aligned} \quad (\text{A17})$$

which yields Eq. (2.10).

Finally, we calculate $\overline{\langle \mathbf{R}_Q^2(L) \rangle}$. This is given by

$$\begin{aligned}
\overline{\langle \mathbf{R}_Q^2(L) \rangle} &= \frac{\int d\mathbf{R}_1 \cdots d\mathbf{R}_n \mathbf{R}_1^2 Z_n(\{\mathbf{R}_a\}, \{\mathbf{R}_a\}; L)}{\int d\mathbf{R}_1 \cdots d\mathbf{R}_n Z_n(\{\mathbf{R}_a\}, \{\mathbf{R}_a\}; L)} \\
&= -\frac{1}{2n} \frac{d}{dU} \ln \int d\mathbf{R}_1 \cdots d\mathbf{R}_n Z_n(\{\mathbf{R}_a\}, \{\mathbf{R}_a\}; L) \\
&= -\frac{1}{2n} \frac{d}{dU} \ln \left[\frac{\pi^n}{[2(U+W)]^{n-1} 2(U+W+2nV)} \right] \\
&= \frac{d}{4} \left(\frac{1}{U+W} - \frac{2V}{(U+W)(U+W+2nV)} \right). \tag{A18}
\end{aligned}$$

In the limit $n \rightarrow 0$ we obtain

$$\begin{aligned}
\overline{\langle \mathbf{R}_Q^2(L) \rangle} &= \frac{d}{4} \left(\frac{1}{U+W} - \frac{2V}{(U+W)^2} \right) \\
&= \frac{d}{\mu^2} \left(\frac{B}{A+C} \right)^2 + \frac{d}{4\beta(A+C)}, \tag{A19}
\end{aligned}$$

which gives rise to Eq. (2.17). $\overline{\langle \mathbf{R}_Q(L) \rangle^2}$ is calculated similarly from $\langle \mathbf{R}_1 \cdot \mathbf{R}_2 \rangle$ and one obtains $4\sigma d/\mu^2$ in agreement with Eq. (2.18).

REFERENCES

- [1] A. Baumgartner and M. Muthukumar, *J. Chem. Phys.* **87**, 3082 (1987).
- [2] S. F. Edwards and M. Muthukumar, *J. Chem. Phys.* **89**, 2435 (1988).
- [3] M. E. Cates and C. Ball, *J. Phys. (France)* **89**, 2435 (1988).
- [4] T. Nattermann and W. Renz, *Phys. Rev. A* **40**, 4675 (1989).
- [5] A. Baumgartner and M. Muthukumar in *Advances in Chemical Physics (vol. XCIV) Polymeric Systems I*. Prigogine and S. A. Rice editors, (John Wiley & Sons, Inc., New York, 1996).
- [6] Y. Y. Goldschmidt, *Phys. Rev. E* **61**, 1729 (2000).
- [7] Y. Y. Goldschmidt, *Phys. Rev. E* **53**, 343 (1996).
- [8] D. R. Nelson and V. M. Vinokur, *Phys. Rev. B* **48**, 13060 (1993).
- [9] Y. Y. Goldschmidt, *Phys. Rev. B* **56**, 2800 (1997).
- [10] G. Parisi, *Rend. Acad. Naz. Lincei* **XI-1**, 3 (1990).
- [11] M. Mezard and G. Parisi, *J. Phys. I France* **1**, 809 (1991).
- [12] M. Mezard, G. Parisi and M. A. Virasoro, *Spin glass theory and beyond* (World Scientific, Singapore, 1987).
- [13] M. Doi and S. F. Edwards, *The Theory of Polymer Dynamics* (Oxford University Press, Oxford, 1986).
- [14] R. P. Feynman, *Statistical Mechanics: A Set of Lectures* (Benjamin, New York, 1972).
- [15] W. H. Press *et al.*, *Numerical Recipes in Fortran*, 2nd ed. (Cambridge University Press 1992).
- [16] H. A. Makse, S. Havlin, H. E. Stanley and M. Schwartz, *CHAOS SOLITON FRACT* **6**, 295 (1995).